SI Appendix for:

High-Resolution Structures of a Heterochiral Coiled Coil

David E. Mortenson, Jay D. Steinkruger, Dale F. Kreitler, Dominic V. Perroni, Gregory P. Sorenson, Lijun Huang, Ritesh Mittal, Hyun Gi Yun, Benjamin R. Travis, Mahesh K. Mahanthappa, Katrina T. Forest, Samuel H. Gellman

Solid-Phase Polypeptide Synthesis

L- and D-peptides of the M2-TM sequence (Ac-PLVVAASIIAILHLILWILDRL-$CONH_2$) were prepared using a microwave-assisted solid-phase synthetic protocol, using standard Fmoc protocols and a CEM MARS 5 microwave reactor. For coupling reactions, 4 equivalents of a given Fmoc- and side-chain protected amino acid, 4 equivalents 2-(6-chloro-1H-benzotriazole-1-yl)-1,1,3,3-tetramethylaminium hexafluorophosphate (HCTU), and 8 equivalents N,N-diisopropylethylamine (DIEA) were pre-activated in N,N-dimethylformamide (DMF; 3 mL per 100 μmol resin loading) and then added to a fritted syringe containing ChemMatrix H-PAL resin (400 μmol/g). The microwave coupling protocol involved a two minute ramp to 70 °C followed by a four-minute hold at that temperature. For Fmoc-deprotection reactions, the resin was suspended in a 20% solution of piperidine in DMF (~2 mL per 25 μmol resin loading), and subjected to a two-minute ramp to 80 °C followed by a two-minute hold at that temperature. All positions in the M2-TM sequence were "double-coupled" – for each coupling reaction, the resin was charged with activated monomer and subjected to microwave heating, and was then drained on a vacuum manifold and subjected to the same reaction conditions again with fresh activated monomer. The resin was washed with DMF and drained (3x) on a vacuum manifold between coupling and deprotection cycles. For double-couplings, the resin was drained but not washed between the two coupling cycles. N-termini were acetylated by shaking the resin in a solution of 8:2:1 (v/v/v) DMF/DIEA/acetic anhydride (11 mL per 100 μmol resin loading); this reaction was carried out

for approximately 10 minutes before washing the resin with DMF. Solid-phase syntheses were typically carried out on 100 μmol scale. Following completion of solid-phase synthesis, the resin was washed extensively with methylene chloride (to remove residual DMF) and dried by forcing compressed air through the syringe or leaving open to atmosphere.

Peptide Cleavage

In preliminary synthetic efforts, crude M2-TM peptides were cleaved from resin in 95/2.5/2.5 TFA/H_2O/TIPS, as described in two previous studies of M2-TM variants (1, 2); however, this cleavage protocol sometimes produced peptide oxidation products as impurities (as evidenced by m/z+16 and m/z+32 peaks in MALDI spectra), even when cleavage reactions were attempted with an N_2 atmosphere. For later synthetic efforts, M2-TM peptides were cleaved from resin using a cocktail containing 81.5% trifluoroacetic acid (TFA), 5% thioanisole, 5% phenol, 5% water 2.5% ethanedithiol and 1% triisopropylsilane; this protocol seemed to suppress oxidative side-reactions and was more straightforward than carrying out cleavage reactions under inert atmosphere. Peptide cleavage was accomplished by suspending the resin in cleavage cocktail (8 mL per 100 μmol resin loading) in a sealed fritted syringe and shaking for 3 hours. Following resin cleavage, the TFA solution was drained into a 50 mL conical tube, the resin was washed 2x with several milliliters of neat TFA, and the combined TFA solutions were evaporated to a volume of several milliliters. Crude peptide mixtures were precipitated by adding 45 mL diethyl ether to fill the conical tube. Solids were collected by centrifuging and decanting away the ether supernatant. Following initial precipitation of the crude peptide mixture, the solids were resuspended in an additional volume of fresh ether, and were centrifuged and collected as described above. Crude samples were dried thoroughly by leaving open to atmosphere for several hours or overnight.

Peptide Purification and Characterization

Following resin cleavage and precipitation of crude M2-TM peptides from diethyl ether, the crude peptide pellets were dissolved in a solution of 1:1 (v/v) TFA:2,2,2-trifluoroethanol (TFE) (800 µL per 100 µmol resin loading) with sonication. These solutions were then diluted to approximately 20 mL total volume (for 100 µmol resin loading) with acetonitrile (MeCN).

Aliquots of crude M2-TM peptides dissolved in the solution described above were purified using a C_5-functionalized reverse-phase column (250 mm x 22 mm; Supelco) heated to 60 °C using a water heater/circulator connected to a column jacket. The binary solvent system used for purifications was H_2O:TFA (100:0.1 v/v) as A solvent and isopropanol:MeCN:H_2O:TFA (60:30:10:0.1 v/v) as B solvent. Following purification, fractions were pooled, diluted into an equal volume of H_2O, and lyophilized to dryness. Polypeptide identity was established using matrix-assisted laser desorption ionization-time of flight (MALDI-TOF) mass spectrometry on a Bruker Ultraflex III mass spectrometer. Calculated $[M+H]^+$ ions are given below assuming monoisotopic mass values. Analytical HPLC runs were carried out to establish peptide purity, and used the same solvent system as described above. Representative characterization data are shown in Supplemental Figures 1 and 2.

L-M2-TM: C_3 analytical column (250 X 4.6 mm, Agilent), flow rate 1 mL/min, 60 °C, gradient 10-90% B solvent in A over 80 minutes, retention time of 74 minutes. MALDI-TOF [M+H]+ calculated 2494.1, observed 2494.2.

D-M2-TM: C_3 analytical column (250 X 4.6 mm, Agilent), flow rate 1 mL/min, 60 °C, gradient 10-90% B solvent in A over 80 minutes, retention time of 74 minutes. MALDI-TOF [M+H]+ calculated 2494.1, observed 2494.1

L-M2-TM

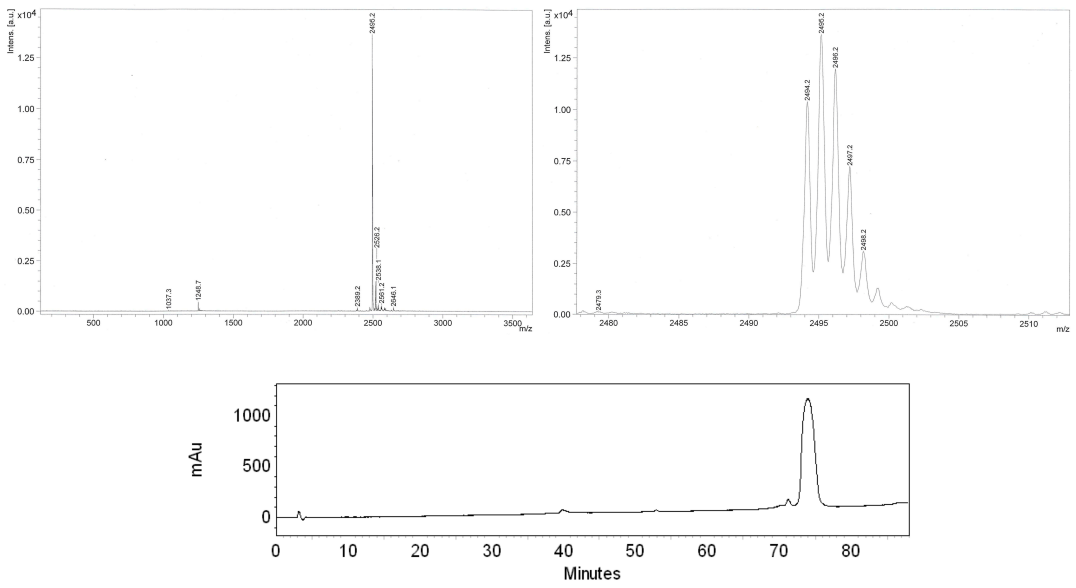

Supplemental Figure 1. HPLC and MALDI mass spectrometric characterization data obtained for L-M2-TM.

D-M2-TM

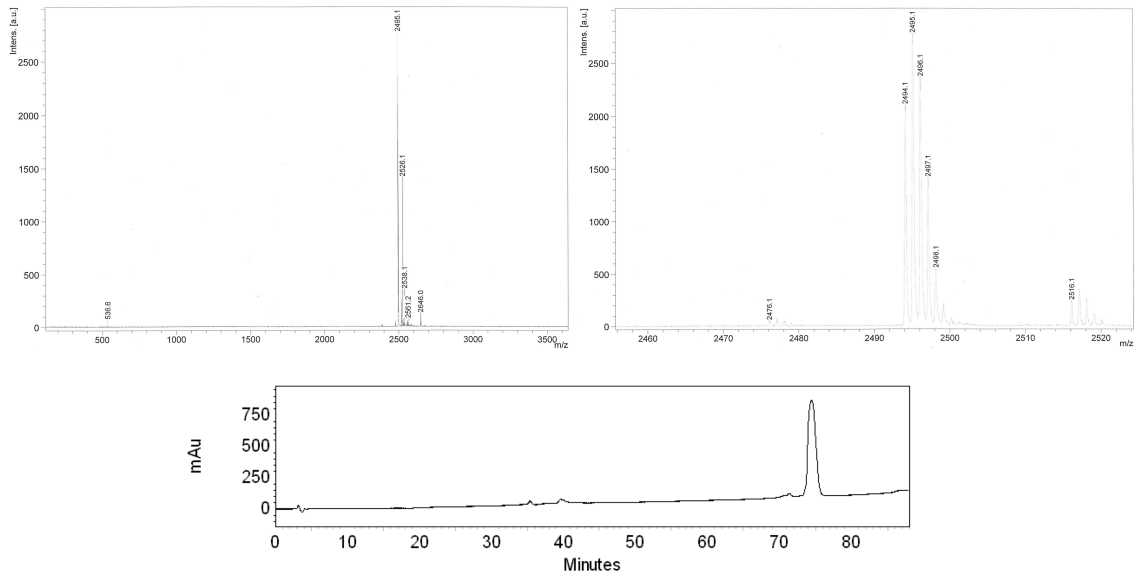

Supplemental Figure 2. HPLC and MALDI mass spectrometry characterization data obtained for D-M2-TM.

M2-TM Crystallization and Diffraction Data Collection

Racemic M2-TM/OG

Stocks of L- and D-OG were each prepared at 2% (w/v) in ultrapure deionized (Milli-Q) water, and were combined to give a 2% stock of racemic OG. L- and D-M2-TM were each dissolved in racemic OG solution, and peptide concentrations were approximated by diluting the stocks of L- and D-M2-TM 20-fold into 8 M guanidinium chloride (GdmCl) solution and measuring the absorbance at 280 nm assuming $\varepsilon_{M2\text{-}TM,280nm}$ = 5690 $M^{-1}cm^{-1}$ (3). L- and D-M2-TM stocks were each diluted to 3 mg/mL concentration and combined in a 1:1 ratio for crystallization experiments. The racemic peptide stock solution became cloudy over time but turned clear again when combined with most of the precipitant solutions used for crystallization trials. Hanging drop vapor diffusion experiments (4) were carried out in Linbro-style plates using the screens MembFac and Crystal Screen II (Hampton Research). For each condition, 1 μL peptide solution was combined with 1 μL precipitant solution on a silanized glass slide, which was then suspended over a 500 μL reservoir volume. Crystals grew overnight from five conditions (22, 42, 43, 46, 48) in Membfac and one condition (40) from Crystal Screen II. Crystals derived from MembFac condition #22 (containing 0.1 M N-(2-acetamido)iminodiacetic acid pH 6.5, 0.1 M ammonium sulfate) were treated with a 3:1 solution of Membfac #22:glycerol prior to vitrification in liquid N_2 and diffraction data collection.

Diffraction data were collected at 100 K using synchrotron radiation (λ = 0 .97872 Å, LS-CAT 21-ID-F). Data collected from two crystals were merged to maximize completeness in both high- and low-resolution data. Indexing, integration and scaling were carried out using the XDS package. The data were cut off at a high-resolution limit of 1.05 Å; this value corresponded to the edge of the detector at the closest possible crystal-to-detector distance. Based on a mean $|E^2\text{-}1|$ = 0.974 (where values of 0.968 and 0.736 are expected for centric and acentric data, respectively), the space group was assigned as $P\bar{1}$.

Five percent of reflections distributed randomly across resolution shells were set aside for the calculation of R_{free}.

While monitoring replicate crystallization experiments involving racemic M2-TM/OG and the precipitant solution gave crystals from sparse-matrix screening (0.1 M ADA pH 6.5 and 1.0 M ammonium sulfate), we noticed large (~500 μm width), strongly birefringent plate-shaped crystals of the racemic form of the detergent OG growing in some experiments (Supplemental Figure 3).

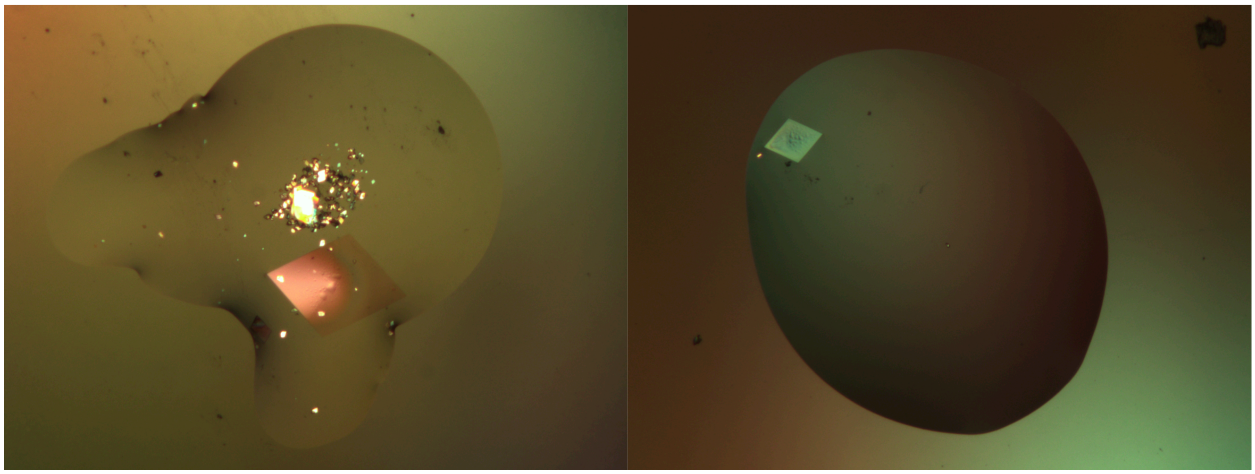

Supplemental Figure 3. Large crystals of racemic OG grown from the precipitant condition used to crystallize racemic M2-TM.

A fragment of a large crystal was briefly treated with 25% glycerol in the precipitant solution described above and was then harvested with a MiTeGen MicroMount® and immediately vitrified in a cryostream. Diffraction data were collected with a Mo microfocus source (λ = 0.709 Å; Bruker). Frames were integrated and scaled in the APEX2 software package, and data were merged in XPREP. On the basis of the $|E^2-1|$ statistic and systematic absences observed for a 2_1 screw axis and *a*/*c* glide, the space group was assigned as $P2_1/c$, which is centrosymmetric. The structure of racemic OG was solved using SHELXS and then refined to convergence in SHELXL (5). The asymmetric unit contains a single molecule of D-OG and an ordered water molecule, while the unit cell contains four copies of OG (2L +

2D) and four ordered waters. This structure has been deposited in the Cambridge Structural Database under accession number CCDC 1058798.

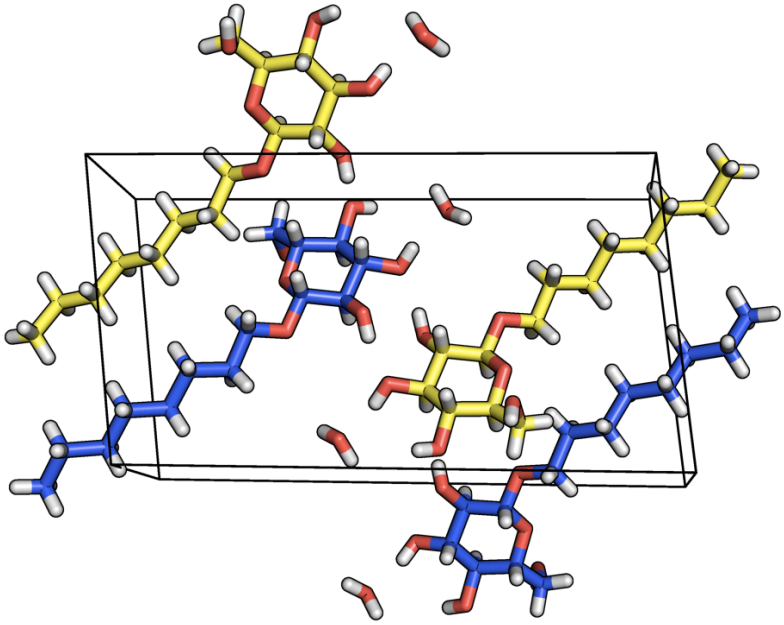

Supplemental Figure 4. Unit cell of racemic OG crystallized in space group $P2_1/c$. D- and L-OG are shown in blue and yellow, respectively.

Racemic M2-TM/LCP

Equal amounts of L- and D-M2-TM peptides were combined with monoolein at 14 - 20% (w/w) peptide loading in lipid by codissolving in 2,2,2,-trifluoroethanol (TFE). This solution was then transferred to a 250 μL gastight syringe (Hamilton) and the solvent was removed gradually using a stream of nitrogen passed through a gel-loading pipette tip. Once most of the TFE had been removed, the syringe was placed under high-vacuum overnight to remove residual solvent. The syringe was fitted to a symmetrical coupler and gently heated over a heat gun until warm to the touch (but not hot) to melt the lipid, and air was then removed from the syringe by passing the plunger up and down and then moving the plunger so that molten lipid was just visible protruding from the end of the coupler needle section. A separate 100 μL gastight syringe was filled with water to produce a 40:60 water/lipid ratio in

the mixed lipid (the mass of peptide added to the lipid was not considered in this ratio), and the two syringes were connected using a syringe coupler apparatus and their contents mixed to produce a uniform gel. The syringes were typically passed back and forth ~100 times before the LCP reached a uniform consistency. LCPs were opaque following mixing, likely due to the high loading of peptide in the lipid. Once the peptide-doped LCP had been mixed to a uniform consistency, one of the syringes was removed from the coupler and replaced with a 10 μL gastight syringe fitted to a ratcheting dispenser (Hamilton), and the 10 μL syringe was filled with LCP. The remaining contents of the larger syringe were then re-sealed for storage.

For preparation of 27-well "sandwich" plates used in crystallization experiments, conventional microscope slides (~25 X 75 mm) were sprayed with Rain-X® windshield treatment several times, until the liquid beaded up on the surface of the glass. Slides were then washed extensively with water and dried. To create 27 "wells" to separate individual crystallization experiments, strips of double-sided adhesive tape that had been cut to the specifications described by Caffrey and Cherezov (6) were affixed to the microscope slides.

Crystallization experiments were carried out by dispensing 200 nL volumes of prepared LCP (*vide supra*) into the 27 "wells" of the microscope slides and adding 1 μL volumes of precipitant solutions from commercially-available screens. LCP was dispensed as close to the middle of the circular wells as possible, and precipitant overlays were dispensed directly on top of the LCP to minimize contact between the precipitant solution and the surrounding adhesive strip. Once nine experiments had been set up in this way (in a 3 X 3 arrangement), this part of the microscope slide was covered with a glass cover slide (25 X 25 mm), and the wells were sealed with the aid of a rubber roller. The remaining wells on the same plate were set up in the same fashion. Small crystals were generally observed within several hours, and larger crystals grew over a period of days to weeks.

The sandwich plates described above were visualized using a stereo microscope to check for crystal growth. In early experiments, we found that the heat resulting from the incandescent light source beneath the stage tended to disrupt the contents of crystallization experiments when plates were visualized after being placed directly on top of the microscope stage. Thus, plates were kept elevated above the microscope stage (using a transparent plastic lid taken from a Linbro plate) to prevent heating of the plates by the microscope light source.

Crystals of racemic M2-TM grown from LCP media were harvested by scoring square-shaped regions of the glass cover slides using a capillary-cutting stone (Hampton Research) and removing sections of glass from above the crystals. Once a region of the cover slide had been separated from the surrounding glass, it was removed with the aid of tweezers. Crystals were harvested using MicroMesh™ mounts (MiTeGen) and were vitrified directly in liquid N_2 without additional cryoprotection. This procedure was carried out in a cold room maintained at 8 °C, as it was found that opening the crystallization experiments at room temperature led to rapid deterioration in the quality of crystals (birefringence under crossed polarizers was observed to dim rapidly once slides were opened at room temperature), likely due to evaporation of water from the LCP/precipitant mixture. Working at lowered temperature allowed more time for crystal manipulation once the crystallization experiments were opened.

Diffraction data were collected at 100 K using synchrotron radiation (λ = 0.97872 Å, LS-CAT 21-ID-F). Indexing, integration, and scaling of the data were carried out using the XDS package (7). The data were truncated at a high-resolution limit of 2.00 Å. Diffraction quality was highly variable with crystal orientation, likely due to the plate-like morphology of the crystals. Setting the parameter DELPHI in the XDS input file (XDS.INP) to a value of 60 frames (the default value is 5 frames) greatly stabilized geometric parameters during data integration; this change to the XDS input was suggested for

difficult data sets on the XDSwiki webpage (http://strucbio.biologie.uni-konstanz.de/xdswiki/index.php/Difficult_datasets). Based on a mean $|E^2-1|$ = 0.951 and systematic absences corresponding to a 2_1 screw axis and *a* glide plane, the space group was assigned as $P2_1/c$, which is centrosymmetric. Five percent of reflections distributed randomly across resolution shells were set aside for the calculation of R_{free}.

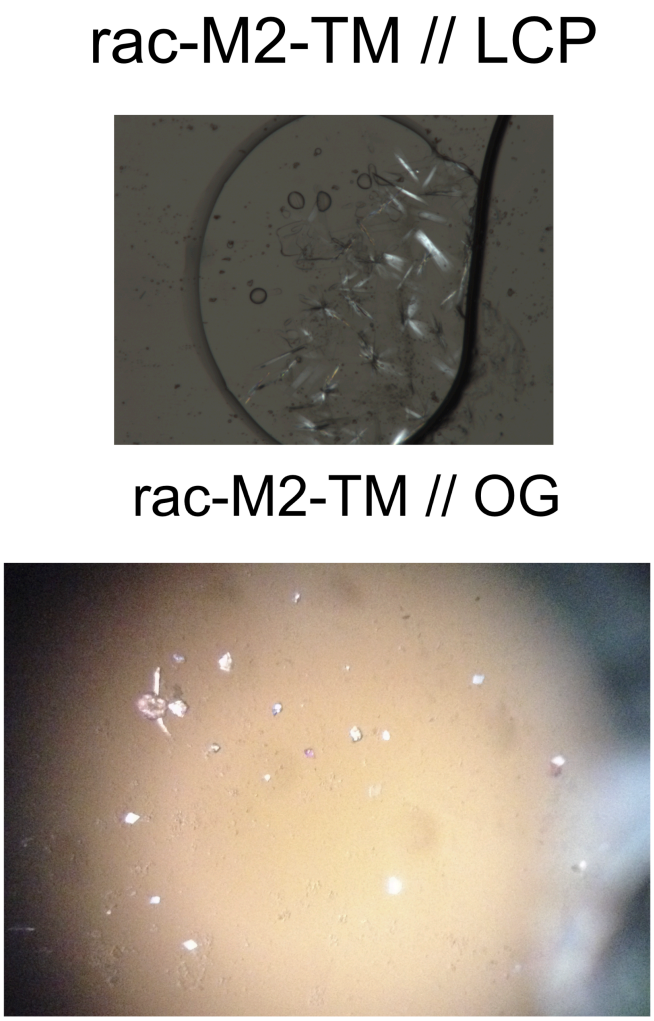

Supplemental Figure 5. Crystals of racemic M2-TM/LCP and racemic M2-TM/OG viewed under partially crossed polarizers.

Small-Angle X-ray Scattering (SAXS) Characterization of Racemic M2-TM/LCP

L- and D-M2-TM were combined with monoolein at 14% total loading (w/w) in lipid. The solvent 2,2,2-trifluoroethanol was evaporated first under a stream of N_2 and then under high vacuum. The resulting solid then was combined with water at a ratio of 60:40 lipid/water. 5 μL LCP was sealed into an aluminum sandwich sample cell fitted with Kapton® polyimide windows. Laboratory source SAXS measurements employed a Bruker Discovery D8 X-ray diffractometer, in which Cu Kα X-rays were focused using a Montell mirror and subjected to pinhole collimation to achieve a final beam diameter of 0.5 mm. Two-dimensional SAXS (2D-SAXS) patterns were recorded on a Vantec 500 area detector (14 cm diameter active area) at a sample-to-detector distance of 45.83 cm (calibrated using a silver behenate standard d = 58.38 Å) with typical exposure times of 15–30 min. Data reduction utilized the DataSqueeze software package (http://www.datasqueezesoftware.com). Azimuthal integration of a 2D-SAXS pattern for the initial peptide-doped LCP furnished a scattered intensity ($I(q)$) versus scattering wavevector (q) profile consistent with the cubic space group symmetry $Pn\bar{3}m$ (space group #224) with a unit cell parameter $\underline{a}$ = 107.1 Å.

Following data collection on the initial state of the peptide-doped LCP, 25 μL of the precipitant solution that had been used to grow diffraction-quality crystals of racemic M2-TM [100 mM ADA pH 6.5, 24% (v/v) MPD] was added to the sample cell. After a 3 h equilibration time, this sample was subjected to SAXS analysis. The resulting 2D-SAXS pattern and associated azimuthally-integrated scattering intensity profile exhibited only a single, broad, low-angle scattering feature consistent with the formation of a L_3-sponge phase.

To ensure that the SAXS measurements described above were representative of the processes involved in peptide crystallization, replicate crystallization experiments were set up in parallel with

SAXS samples using the same stocks of peptide-doped LCP and precipitant solution. These experiments afforded crystals within one hour.

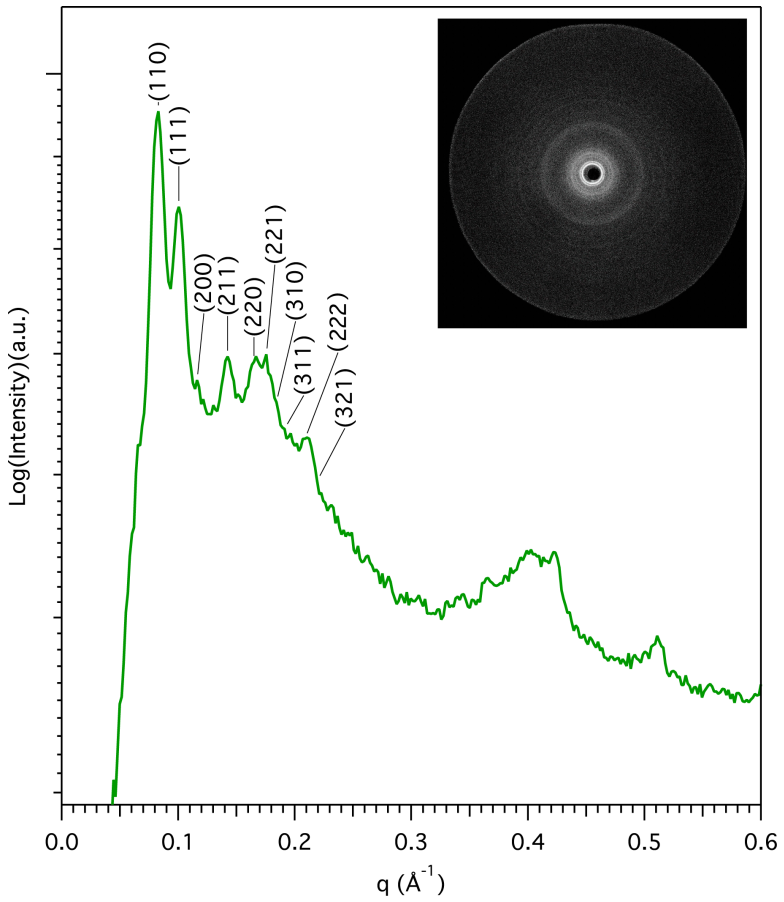

Supplemental Figure 6. Azimuthally-integrated SAXS intensity profile and 2D-SAXS pattern (*inset*) obtained from a sample of racemic M2-TM-doped monoolein LCP prior to treatment with the precipitant solution used for crystallization studies. This scattering pattern is consistent with a bicontinuous cubic phase having $Pn\bar{3}m$ (space group #224) symmetry with a unit cell parameter a = 107.1 Å. The positions of the calculated SAXS peak maxima are given along with the associated Miller indices (*hkl*) for the first ten expected reflections. The broad peak observed at ~0.4 Å is an artifact arising from the Kapton® windows of the sample cell used for this measurement.

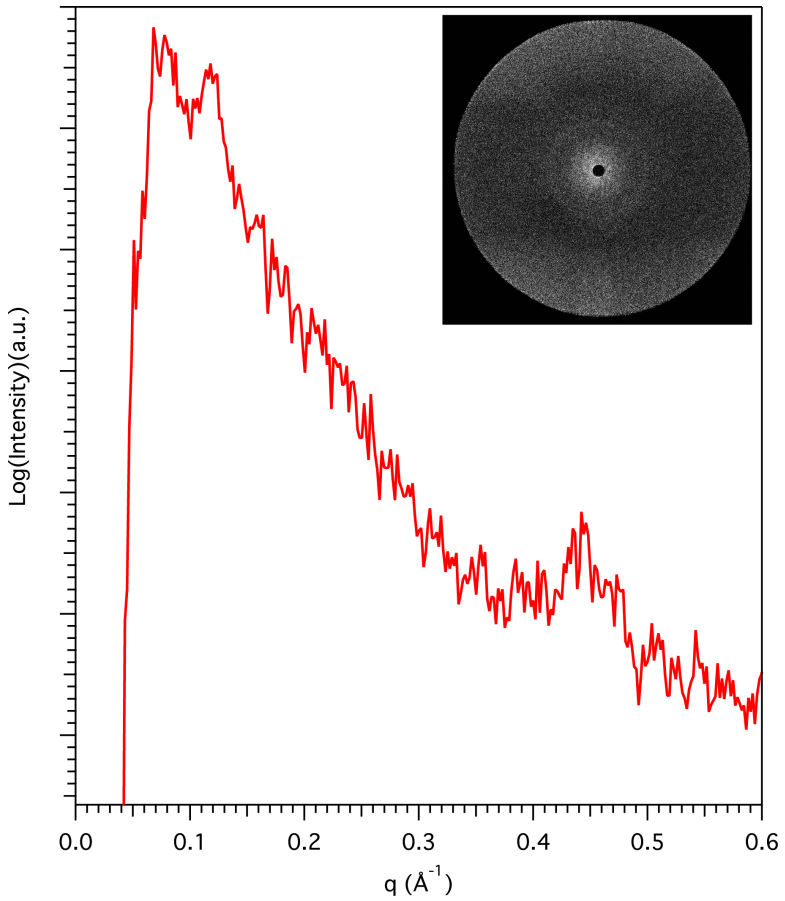

Supplemental Figure 7. Azimuthally-integrated SAXS intensity profile and 2D-SAXS pattern (*inset*) obtained from a sample of racemic M2-TM-doped monoolein LCP 3 hours after treatment with the precipitant solution used for crystallization studies. In contrast to the SAXS pattern collected prior to the addition of the precipitant solution, the absence of any higher order SAXS peaks beyond the broad peak centered at low *q* indicates that the precipitant induces a lyotropic phase transition to a more disordered structure, tentatively assigned as a L_3-sponge phase. The peak observed at ~0.4 Å is an artifact arising from the Kapton® windows of the sample cell used for this measurement.

M2-TM Structural Solution and Model Refinement

Racemic M2-TM/OG

The structure of racemic M2-TM/OG was initially solved using a data set collected on a rotating anode source to a high-resolution limit of 2.2 Å. The structure was solved by molecular replacement in PHASER (8) using a single helix derived from the structure of racemic M2-TM/LCP (*vide infra*) as a search model. After solving and partially refining against lab source-derived data, the model of racemic M2-TM/OG was then refined against synchrotron data at 1.05 Å resolution, carrying over the same set of reflections that had previously been flagged for the calculation of R_{free}. The structure was refined *via* maximum likelihood methods in Refmac5 (9) using anisotropic thermal parameters and hydrogen atoms included at riding positions (Supplemental Table 1). Model refinement converged at values of R/R_{free} of 0.138/0.156. Given the expectation that centric reflection data are more broadly distributed than acentric data, these R-values are equivalent to R/R_{free} of 0.088/0.101 for a non-centrosymmetric model with a similar degree of coordinate error (10).

For some residues in the M2-TM sequence, alternate conformations were modeled after positive F_O-F_C density corresponding to multiple side chain rotamers was observed at these positions. For the C-terminal Leu46 residue, modeling two conformations of the side chain alone did not produce a good fit to the observed electron density, and it appeared that the entire residue, including the C-terminal amide, was disordered over at least two states. A composite omit map was generated after removing Leu46 and the C-terminal amide functional group from the model; inspection of this map revealed $2F_O$-F_C and positive F_O-F_C density corresponding to two major conformations of the C-terminal amide. For subsequent refinements, both the Leu46 side chain and the C-terminal amide group were split over two conformations.

Racemic M2-TM/LCP

The structure of racemic M2-TM/LCP was initially solved using a data set collected on a rotating anode source, to a high-resolution limit of 2.27 Å. The structure was solved by molecular replacement in PHASER (8) using a single helix derived from a previously reported structure of M2-TM (PDB: 3LBW) as a search model. The model was initially refined against lab source-derived data and was then re-refined against synchrotron data at a high-resolution limit of 2.0 Å, using the same set of reflections that had previously been flagged for the calculation of R_{free}. This structure was refined *via* maximum likelihood methods in Refmac5 (9) using isotropic thermal parameters and hydrogen atoms included at riding positions (Supplemental Table 1). Model refinement of the structure of racemic M2-TM/LCP converged at values of R/R_{free} of 0.281/0.296. Given the relationship between centric and acentric reflection data described above, these values correspond to R/R_{free} of 0.190/0.201 for an acentric model with similar coordinate error (10). Although the conformations of the two symmetry-independent copies of L-M2-TM are closely related (RMSD over all Cα: 0.1 Å), they differ in the conformation of residue Arg45. In one chain, this residue makes a salt-bridging contact with Asp44 from a nearby copy of D-M2-TM, while in the other chain, the side chain of Arg45 appears to form a hydrogen bond with the amide carbonyl of Asp44 from D-M2-TM.

Supplemental Table 1.

	Racemic M2-TM/OG (4RWC)	Racemic M2-TM/LCP (4RWB)
Data Collection Temp. (K)	100	100
Beamline/Detector	21-ID-F	21-ID-F
Wavelength (Å)	0.97872	0.97872
Resolution range	26.59 – 1.05 (1.08 – 1.05)*	19.39 – 2.00 (2.03 – 2.00)
Unique reflections	17458 (983)	6119 (442)
Completeness (%)	92.6 (65.9)	96.2 (95.9)
$R_{sym/merge}$	0.072 (0.381)	0.127 (0.560)
I/σ(I)	12.9 (2.9)	8.9 (2.3)
Redundancy	6.0 (2.5)	7.1 (7.2)
Wilson B-factor (Å^2)	5.3	17.3
Space group	$P\bar{1}$	$P2_1/c$
Unit cell parameters		
(a/b/c) (Å)	15.4/25.9/27.0	40.9/41.2/27.9
(α / β / γ) (°)	90.0/99.5/99.9	90/95.7/90
Refinement:		
# Non-H Atoms	241	433
Resolution range (Å)	26.59 – 1.05	19.39 – 2.00
R(work)	0.138 (0.242)	0.281 (0.333)
R(free)	0.156 (0.201)	0.296 (0.306)
RMS bond length (Å)	0.019	0.019
RMS bond angle (°)	2.1	2.1
Coordinate ESU (Å)	0.012	0.110
Mean B Value (Å^2)	14.7	28.4

*Values in parentheses are reflections in the highest-resolution shell.

Center-of-Mass Distance Calculations

Side chain mean coordinates were calculated in PyMol using a Python script (available for download at https://raw.githubusercontent.com/Pymol-Scripts/Pymol-script-repo/master/center_of_mass.py; author: Sean Law, PhD, Michigan State University). Values were calculated using only heavy atom positions (i.e., C, N, O), and were not weighted in terms of atomic mass; thus, these values may also be described as "centers-of-geometry". This method is consistent with the protocol implemented in SOCKET by Walshaw and Woolfson (11). The script described above was used to generate pseudoatoms at positions calculated for all side chains, and the distances between these markers were calculated using the *dist* function in PyMol (12). For side chains that were modeled as multiple rotameric conformations mean coordinates were calculated using the positions of atoms from all conformations.

References

1. Stouffer AL *et al*. (2008) Structural basis for the function and inhibition of an influenza virus proton channel. *Nature* 451(7178): 596-599.

2. Acharya R *et al*. (2010) Structure and mechanism of proton transport through the transmembrane tetrameric M2 protein bundle of the influenza A virus. *Proc Natl Acad Sci USA* 107(34): 15075-15080.

3. Edelhoch H (1967) Spectroscopic determination of tryptophan and tyrosine in proteins. *Biochemistry* 6(7): 1948-1954.

4. McPherson A (1982) Preparation and analysis of protein crystals. *Chichester: John Wiley*.

5. Sheldrick GM (2008) A short history of SHELX. *Acta Cryst* A64(1): 112-122.

6. Caffrey M, Cherezov V (2009) Crystallizing membrane proteins using lipidic mesophases. *Nature Prot* 4(5): 706-731.

7. Kabsch W (2010) XDS. *Acta Cryst* D66(2): 125-132.

8. McCoy AJ *et al*. (2007) Phaser crystallographic software. *J Appl Cryst* 40(4): 658-674.

9. Murshudov GN, Vagin AA, and Dodson EJ (1997) Refinement of macromolecular structures by the maximum-likelihood method. *Acta Cryst* D53(3): 240-255.

10. Luzzati PV (1952) Traitement statistique des erreurs dans la determination des structures cristallines. *Acta Cryst* D5(6): 802-810.

11. Walshaw J, Woolfson DN (2001) Socket: a program for identifying and analyzing coiled-coil motifs within protein structures. *J Mol Biol* 307(5): 1427-1450.

12. MacPyMOL v1.5.0.4, Schrödinger, LLC.